

Spin phase diagram of the $\nu_e=4/11$ composite fermion liquid

Arkadiusz Wójs,^{1,2} George Simion,² and John J. Quinn²¹*Institute of Physics, Wrocław University of Technology, Wybrzeże Wyspiańskiego 27, 50-370 Wrocław, Poland*²*Department of Physics, University of Tennessee, Knoxville, Tennessee 37996, USA*

(Received 8 January 2007; revised manuscript received 26 February 2007; published 13 April 2007)

Spin polarization of the “second-generation” $\nu_e=4/11$ fractional quantum Hall state (corresponding to an incompressible liquid in a one-third-filled composite fermion Landau level) is studied by exact diagonalization. A spin phase diagram is determined for GaAs structures of different widths and electron concentrations. Transition between the polarized and partially unpolarized states with distinct composite fermion correlations is predicted for realistic parameters.

DOI: [10.1103/PhysRevB.75.155318](https://doi.org/10.1103/PhysRevB.75.155318)

PACS number(s): 71.10.Pm, 73.43.-f

I. INTRODUCTION

There has been considerable speculation about the nature of “second-generation” incompressible quantum liquid (IQL) states observed recently by Pan *et al.*¹ Their incompressibility depends on spin and charge dynamics of the fractionally charged Laughlin quasiparticles (QPs).²

The experiment of Pan *et al.* employed the fractional quantum Hall (FQH) effect,³ a nonperturbative interaction many-body phenomenon, dependent on magnetic quantization of the two-dimensional single-electron energy spectrum into massively degenerate Landau levels (LLs).⁴ It coincides with the formation of electron IQLs and thus occurs at the particular fractional values of the LL filling factor, defined as $\nu_e=2\pi\varrho_e\lambda^2$ [where ϱ_e is the electron concentration and $\lambda=(\hbar c/eB)^{1/2}$ is the magnetic length].

The emergence of IQLs is explained as follows by the composite fermion (CF) theory.⁵ Electrons partially filling the lowest LL are said to capture $2p$ magnetic flux quanta $\phi_0=\hbar c/e$ and become (weakly interacting) CFs moving in a reduced effective magnetic field, corresponding to a higher effective CF filling factor ν_{CF} . The most prominent IQL sequence at $\nu_e=s(2ps\pm 1)^{-1}$ (with s and p being a pair of integers) corresponds to $\nu_{CF}=s$, i.e., to the integral quantum Hall effect of the CFs.

However, not all IQLs found in the lowest LL can be explained in this way. Recently, Pan *et al.*¹ observed the FQH effect at $\nu_e=4/11$, corresponding to $\nu_{CF}=4/3$, i.e., to a partial filling of a CF-LL. This discovery demonstrated that CFs, like electrons, can form IQLs. The origin of incompressibility of the correlated CF liquid of Pan *et al.* (also called a second-generation FQH state) has been vigorously studied for the last three years.^{6–12} However, some of even the most fundamental questions remain controversial.

The subject of this paper is polarization of the $\nu_e=4/11$ state. It is largely motivated by the wealth of theory of spin dynamics in the “first-generation” FQH states.^{13–20} However, our main goal is to extend the work of Chang *et al.*²¹ and directly address the experimental results of Pan *et al.* in tilted magnetic fields¹ which indicated ferromagnetic order. In the CF picture, this corresponds to a completely filled lowest CF-LL ($0\downarrow$) and a $1/3$ -filled first excited CF-LL with the same spin ($1\uparrow$). Since the Laughlin $\nu=1/3$ state in CF-LL₁ was earlier ruled out²² based on the form of short-range CF-CF in-

teraction pseudopotential, the explanation for the observed incompressibility must be different. This distinction makes the polarized $\nu_e=4/11$ state an object of intense investigation.²³ Although several ideas were formulated (e.g., CF pairing^{9,11}), neither an analytic CF wave function nor an intuitive understanding for the incompressibility has been reached. A partially unpolarized state was also proposed,²⁴ with the $\nu=1/3$ filling of the lowest CF-LL with reversed spin ($0\downarrow$). In contrast to the polarized state and due to a different form²⁵ of CF-CF interaction in CF-LL₀, it is expected to be a Laughlin CF liquid. However, this state has not yet been observed in experiment.

Let us summarize this remarkable situation as follows: The polarized state has been observed but it is not well understood, and the unpolarized state has not been observed but it appears to be much easier to understand. In this paper, we calculate the single-particle and correlation energies in these two competing CF states, depending on the experimentally controlled parameters (electron layer width, concentration, and magnetic field). The main result is the spin phase diagram, from which we predict a spin transition at $\nu_e=4/11$, induced, e.g., by an additional electric field narrowing the electron layer. Suggested experimental demonstration of this transition would shed more light on the role played by spin of correlated CFs.

II. NUMERICAL MODEL

The calculations were done in Haldane’s spherical geometry,²⁶ convenient for the numerical studies of incompressible quantum liquids with short-range correlations. To model an extended (planar) two-dimensional (2D) system of interacting particles filling a fraction ν of a degenerate LL, their finite number N is considered within a shell of appropriate angular momentum l and degeneracy $g=2l+1$ (containing states with different angular momentum projections, $|m|\leq l$). The assignment of the filling factor ν to a finite system (N, g) is not trivial. It requires identifying the dependence $g=\nu^{-1}N+\gamma$ which defines a series of finite systems representing an infinite state ν (here, the “shift” γ is independent of N but it depends on the form of correlations, i.e., in particular, on ν).

In the original formulation,^{26,27} these l shells represent LLs of a charged particle confined to a surface of a sphere of

radius R , with the normal magnetic field B produced by a Dirac monopole of strength $2Q=4\pi R^2 B/\phi_0$. Specifically, the n th LL on a plane (called LL_n , with $n \geq 0$) corresponds to the shell of $l=Q+n$ on a sphere.

Here, we do not use the particular form of the $|Q;n,m\rangle$ wave functions but take advantage of the fact that the symmetry of angular momentum eigenstates $|l,m\rangle$ under 2D rotations mimics the symmetry of the planar eigenstates under 2D (magnetic) translations. Thus, the interaction matrix elements are guaranteed to obey general rules for a scalar operator in the basis of spherical harmonics, but the particular values are put into the model “by hand,” so as to describe the actual interaction among the considered particles (on the plane). This is done by specifying the Haldane pseudopotential,²⁸ defined as interaction energy V as a function of relative angular momentum \mathcal{R} . On a sphere, relative and total pair angular momenta are related by $\mathcal{R}+L=2l$, and the matrix elements $\langle l_1, m_1; l_2, m_2 | V | l_3, m_3; l_4, m_4 \rangle$ are connected with $V(L)$ through the Clebsch-Gordan coefficients.

The many-body interaction Hamiltonian is diagonalized numerically in the configuration-interaction basis. The energy levels E are determined separately for each subspace of the total spin S and angular momentum L .

III. SINGLE-QUASIELECTRON ENERGIES

In the mean-field CF transformation, the liquid of correlated electrons at $\nu_e = \frac{4}{11}$ is converted to the system of CFs with an effective filling factor $\nu_{CF} = \frac{4}{3}$. Thus, the low-energy dynamics of N_e electrons with Coulomb interaction in the lowest LL can be mapped onto that of $\sim \frac{3}{4}N_e$ CFs completely and rigidly filling the lowest CF-LL ($0\uparrow$) and the excess of $N \approx \frac{1}{4}N_e$ CFs in the $\nu = \frac{1}{3}$ -filled next lowest CF-LL (either $1\uparrow$ or $0\downarrow$, depending on the relative magnitude of electron Zeeman energy E_Z and the effective CF cyclotron gap $\propto e^2/\lambda$). Each CF in the partially filled $1\uparrow$ or $0\downarrow$ LL represents a “normal”² or “reversed-spin”¹⁵ quasielectron (QE or QE_R) of the underlying incompressible Laughlin liquid, respectively.

The Coulomb energies ε_{QE} and ε_{QE_R} of these two QPs can be extracted^{25,27} from exact diagonalization of finite systems of N_e electrons in the lowest LL with the appropriate degeneracy g . The Laughlin ground state occurs at $g=3N_e-2 \equiv g_L$; it is nondegenerate ($L=0$) and spin polarized ($S = \frac{1}{2}N_e$). A single QE or QE_R appears in the Laughlin liquid in the lowest states at $g=g_L-1$ and either $S=\frac{1}{2}N_e$ or $\frac{1}{2}N_e-1$, respectively. The QE and QE_R energies ε (defined relative to the underlying Laughlin liquid) are obtained from the comparison of the (N_e -electron) energies at $g=g_L$ and g_L-1 .

The numerical procedure and the result for an ideal 2D electron layer were presented earlier.^{25,27} In Fig. 1, we compare the QE/ QE_R energies calculated for quasi-2D layers of finite width w . Here, w is the effective width of the electron wave function in the normal (z) direction, approximated by $\chi(z) \propto \cos(z\pi/w)$. It is slightly larger than the quantum well width W ; e.g., for symmetric GaAs/ $Al_{0.35}Ga_{0.65}As$ wells, $w \approx W+3$ nm over a wide range of $W \geq 10$ nm. The regular dependence on system size in Fig. 1(a) allows reliable extrapolation of ε to $N_e^{-1} \rightarrow 0$ (planar geometry). From the com-

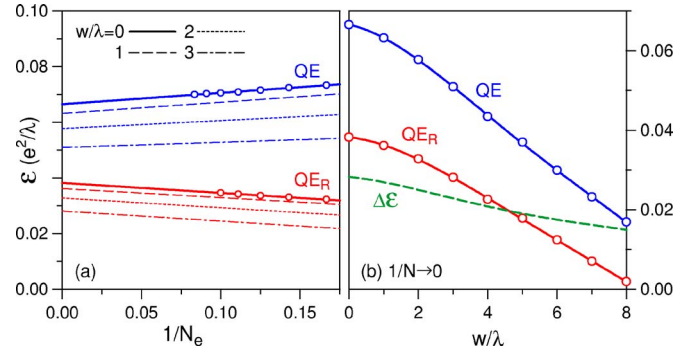


FIG. 1. (Color online) Dependence of the quasielectron (QE) and reversed-spin quasielectron (QE_R) energies ε on (a) the inverse electron number N_e^{-1} in a finite-size calculation and (b) the electron layer width w . λ is the magnetic length.

parison of $\varepsilon_{QE}(w)$ and $\varepsilon_{QE_R}(w)$ in Fig. 1(b), it is clear that their difference $\Delta\varepsilon$ is less sensitive to the width than any of the ε . To put the shown width range in some perspective, let us note that a (fairly narrow) $W=12$ nm well in a (fairly low) field $B=10$ T corresponds to $w/\lambda=1.9$ and $\Delta\varepsilon(w)/\Delta\varepsilon(0)=0.9$, justifying the 2D approximation. On the other hand, a wide $W=40$ nm well in a high field $B=23$ T gives $w/\lambda=8.1$ and $\Delta\varepsilon(w)/\Delta\varepsilon(0)=0.5$, i.e., a significant width effect.

IV. QUASIELECTRON INTERACTIONS

The weak effective CF-CF interactions are known with some accuracy from earlier studies.^{11,22,25,29,30} At least at sufficiently low CF fillings factors $\nu \leq \frac{1}{3}$, they can be well approximated by fixed Haldane pseudopotentials (independent of the CF-LL filling or spin polarization). The short-range QE-QE, QE_R - QE_R , and QE- QE_R pseudopotentials can be obtained from finite-size diagonalization for N_e electrons with up to two reversed spins ($S=\frac{1}{2}N_e-2$) at $g=g_L-2$.

The result is a reliable account of the relative values $\Delta V_{\mathcal{R},\mathcal{R}'} = V(\mathcal{R}) - V(\mathcal{R}')$ at small neighboring \mathcal{R} and \mathcal{R}' , but the absolute values are not estimated very accurately. Fortunately, since vertical correction of $V(\mathcal{R})$ by a constant does not affect the many-CF wave functions and only rigidly shifts the entire energy spectrum, a few leading values of ΔV completely determine the (short-range) CF correlations at a given ν . Therefore, the knowledge of those few approximate values of ΔV_{QE_R} and ΔV_{QE} was sufficient to establish that (i) the QE_R s form a Laughlin $\nu = \frac{1}{3}$ liquid,^{21,24,25} which in finite N - QE_R systems on a sphere occurs at $g=3N-2$, and (ii) in contrast, the QEs form a different (probably paired) state^{9,11} at the same $\nu = \frac{1}{3}$, which, on a sphere, occurs at $g=3N-6$.

However, the relative strength of QE-QE and QE_R - QE_R pseudopotentials V_{QE_R} and V_{QE} must be also known (in addition to ΔV) to compare the energies of many- QE_R and many-QE states (i.e., of the spin-polarized and unpolarized electron states at $\nu_e = \frac{4}{11}$). The absolute values of V_{QE_R} and V_{QE} can be obtained by matching²⁹ the short-range behavior from exact diagonalization of small systems with the long-range behavior predicted for a pair of charges $q = -\frac{1}{3}e$. Specifically, the short-range part of $V_{QE_R}(\mathcal{R})$, which describes a

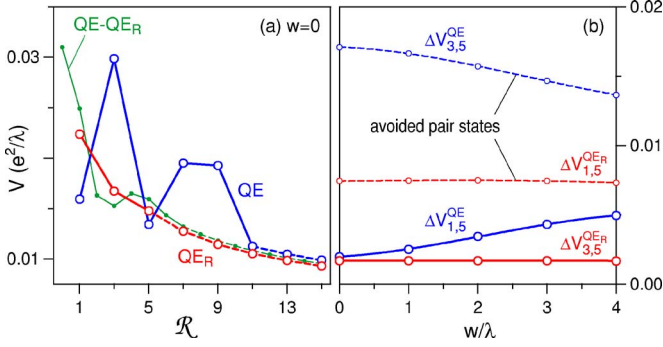


FIG. 2. (Color online) (a) Haldane pseudopotentials (pair interaction energy V as a function of relative angular momentum \mathcal{R}) for quasielectrons (QE) and reversed-spin quasielectrons (QE_R) in an ideal 2D ($w=0$) electron layer. (b) Dependence of pseudopotential increments $\Delta V_{\mathcal{R}\mathcal{R}'} = V(\mathcal{R}) - V(\mathcal{R}')$ on the electron layer width w . λ is the magnetic length.

pair of CFs in the $1\downarrow$ CF-LL, is shifted to match $\eta V_0(\mathcal{R})$, the electron pseudopotential in the lowest LL rescaled by $\eta \equiv (q^2 \lambda_q^{-1}) / (e^2 \lambda_e^{-1}) = (q/e)^{5/2}$. Similarly, the short-range part of $V_{QE}(\mathcal{R})$, related to the $1\uparrow$ CF-LL, is shifted to match $\eta V_1(\mathcal{R})$.

The result in Fig. 2(a) for an ideal 2D layer was reported earlier;¹¹ in Fig. 2(b), the width dependence of the leading parameters ΔV has been plotted. It is noteworthy that V_{QE} is much more sensitive to the electron layer width w than V_{QE_R} . This is explained by stronger oscillations in $V_{QE}(\mathcal{R})$ at $w=0$, which tend to weaken in wider wells (when the characteristic in-plane distances decrease relative to w). The curves for $V_{QE_R}(1)$ and $V_{QE}(3)$ have been drawn with dashed lines, since the QE_R - QE_R and QE - QE pair states associated with these dominant pseudopotential parameters will be avoided⁹ in the unpolarized and polarized $\nu=1/3$ CF ground states, respectively.

V. CORRELATION ENERGIES OF QUASIELECTRON LIQUIDS

As mentioned above, due to the strong QE_R - QE_R repulsion at short range ($\mathcal{R}=1$), the QE_R s form a Laughlin $\nu=1/3$ state similarly to the electrons at $\nu_e=1/3$. The corresponding series of nondegenerate N - QE_R ground states on a sphere occurs at the Laughlin sequence of $g=3N-2$. In Fig. 3(a), we plot the size dependence of their correlation energy u (per particle), defined as

$$u = \frac{E + U_{\text{bckg}}}{N} \zeta. \quad (1)$$

Here, E is the interaction energy of the ground state of N QE_R s and $U_{\text{bckg}} = -(Nq)^2/2R$ is a correction due to interaction with the charge-compensating background (with the sphere radius $R = \lambda\sqrt{Q}$ taken for $2Q+1=g$, in analogy to the relation for electrons in the lowest LL). The factor $\zeta = \sqrt{Q(Q-1)^{-1}}$ is used to rescale the energy unit $e^2/\lambda = \sqrt{Q}e^2/R$ from that corresponding to $g_{QE_R} = 3N-2$ to that of an average $\bar{g} = \frac{1}{2}(g_{QE_R} + g_{QE}) = 3N-4$, to allow for a later com-

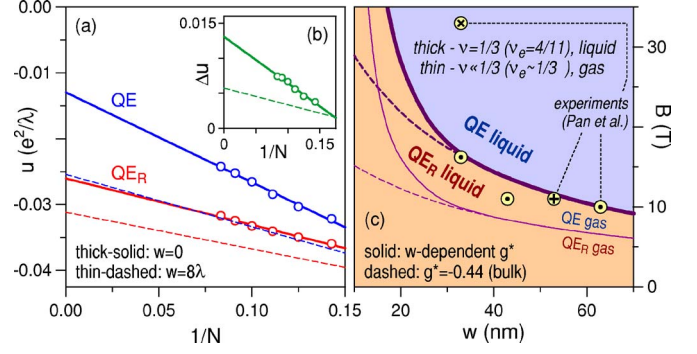


FIG. 3. (Color online) (a) Correlation energy u in the $\nu=1/3$ incompressible liquid of quasielectrons (QE) or reversed-spin quasielectrons (QE_R) as a function of their inverse number N^{-1} for two different widths w of the quasi-2D electron layer (λ is the magnetic length). (b) Difference $\Delta u = u_{QE} - u_{QE_R}$ as a function of N^{-1} . (c) Phase diagram (critical layer width w vs magnetic field B) for the QE - QE_R spin transition at $\nu=1/3$ (i.e., at $\nu_e=4/11$), assuming the effective electron Landé g^* factor for GaAs (dashed line is for the bulk value $g^* = -0.44$, ignoring dependence on the layer width w). Thin lines are for uncorrelated QEs or QE_R s (at $\nu \ll 1/3$). The experimental points were taken after Pan *et al.* (the plus, cross, and dots after Refs. 1, 31, and 32, respectively).

parison of u calculated for QE_R s and QEs at different g (and thus, at different magnetic lengths λ corresponding to the same area $4\pi R^2$).

The correlation energies u were calculated for $N \leq 12$ and extrapolated to $N^{-1} \rightarrow 0$ to eliminate the finite-size effects. Neither the particular form of U_{bckg} (i.e., the assumption of $g=2Q+1$ for the relation between R and λ) nor the rescaling by ζ directly affects the extrapolated value (they only affect the size dependence, and thus the accuracy of extrapolation). For an ideal 2D system, the result of extrapolation is $u_{QE_R} = -0.026e^2/\lambda = -0.405\eta e^2/\lambda$. This value is very close to ηu_0 , where $u_0 = -0.412e^2/\lambda$ describes the Laughlin state of electrons in LL_0 . Good agreement confirms not only Laughlin correlations among the QE_R s (which are guaranteed by the form of ΔV_{QE_R} and can also be verified directly by the analysis of pair amplitudes) but, more importantly, the accurate estimate of the absolute values of $V_{QE_R}(\mathcal{R})$ drawn in Fig. 2(a) and used in the N - QE_R calculation.

Let us turn to the QEs. The dominant QE - QE repulsion at $\mathcal{R}=3$ causes the QEs to form pairs¹¹ rather than a Laughlin state at $\nu=1/3$ (although the exact wave function of this incompressible state is still unknown). The corresponding series of nondegenerate N - QE ground states on a sphere was identified⁹ at $g=3N-6$, different from the Laughlin sequence. The QE correlation energy u was calculated from the same Eq. (1) but with a different $\zeta = \sqrt{Q(Q+1)^{-1}}$ (where $g=2Q+1$ also). By using different ζ_{QE_R} and ζ_{QE} , we removed the discrepancy between λ/R of finite N - QE_R and N - QE systems, in order to improve size convergence of $\Delta u = u_{QE} - u_{QE_R}$.

In an ideal 2D system ($w=0$), the extrapolated value at $N^{-1}=0$ is $u_{QE} = -0.013e^2/\lambda$, twice smaller (in the absolute value) than u_{QE_R} of a Laughlin state. The difference $\Delta u = 0.013e^2/\lambda$ is the key numerical result of this paper. The

accuracy of this estimate can be judged from the extrapolation plot in Fig. 3(b).

The fact that $u_{\text{QE}_R} < u_{\text{QE}}$ can be explained from the comparison¹¹ of QE_R and QE charge-density profiles $\rho(r)$. The roughly Gaussian ρ_{QE_R} is (up to normalization) very similar to ρ_0 of an electron in the lowest LL, yielding similar QE_R and electron pseudopotentials $V(\mathcal{R})$ and correlation energies u (in the η -rescaled units). The ringlike ρ_{QE} is more complicated and has a bigger radius, causing stronger (on the average) QE-QE repulsion. The estimate of how much stronger depends on the accurate matching of the short- and long-range QE-QE pseudopotentials in Fig. 2(a). Therefore, to gain more confidence, we compared u_{QE_R} with u_1 of the electrons filling $\nu = \frac{1}{3}$ of LL_1 , whose ρ_1 falls between $\rho_{\text{QE}_R} \sim \rho_0$ and ρ_{QE} in terms of occupied area and the number of oscillations. For the known³³ $g = 3N - 6$ sequence of nondegenerate $\nu = \frac{1}{3}$ ground states in LL_1 , we obtained $u_1 = -0.32e^2/\lambda$. Upon rescaling for the fractional QP charge, $\eta u_1 = -0.021e^2/\lambda$ falls between $\eta u_0 \approx u_{\text{QE}_R} = -0.026e^2/\lambda$ and $u_{\text{QE}} = -0.013$. This demonstrates that the difference between u_{QE_R} and u_{QE} is caused by the difference between ρ_{QE_R} and ρ_{QE} and supports the obtained order of magnitude of Δu .

To demonstrate the dependence of the correlation energies on layer width, we also showed data for $w = 8\lambda$ in Figs. 3(a) and 3(b). The extrapolated values for this very wide layer are $u_{\text{QE}_R} = -0.025e^2/\lambda$ and $u_{\text{QE}} = -0.031e^2/\lambda$. Significant decrease of both energies compared to $w = 0$ reflects an overall (averaged over in-plane distances, i.e., over \mathcal{R}) reduction of the QP repulsion in wider wells caused by the spread of electron (and thus also QE_R and QE) wave functions in the z direction. Due to different in-plane dynamics, u_{QE_R} and u_{QE} depend differently on width, and their difference $\Delta u = 0.06e^2/\lambda$ at $w = 8\lambda$ is about twice smaller than that at $w = 0$.

VI. SPIN PHASE DIAGRAM FOR $\nu_e = 4/11$

Whether QEs or QE_R s will form a $\nu = \frac{1}{3}$ state at $\nu_e = \frac{4}{11}$ depends on the competition of Coulomb and Zeeman energies. The condition for the $\text{QE} \leftrightarrow \text{QE}_R$ transition is

$$\Delta\varepsilon + \Delta u = E_Z. \quad (2)$$

The competing phases differ in electron-spin polarization ($P = 100\%$ vs 50%). They are both incompressible but probably have different excitation gaps (and thus might not show equally strong FQH effect). In an ideal 2D electron layer, the excitation gap (for neutral excitations) of the polarized state can be expected⁹ below $0.005e^2/\lambda$, and, for the Laughlin state of QE_R s, it is estimated at $\sim 0.06\eta e^2/\lambda = 0.004e^2/\lambda$ (note, however, that a much smaller value of $\sim 0.001e^2/\lambda$ was predicted in Ref. 21). The nature of charged excitations and the corresponding transport gaps (especially in more realistic conditions, i.e., for $w > 0$, including LL mixing and disorder, etc.) are not known, and their prediction should require a much more extensive calculation.

Let us concentrate on the question of stability of either QE_R s or QEs at $\nu_e = \frac{4}{11}$. In order to draw the phase diagram for GaAs heterostructures in Fig. 3(c), we combined the es-

timated dependences of $\Delta\varepsilon/(e^2\lambda^{-1})$ and $\Delta u/(e^2\lambda^{-1})$ on w/λ (where $e^2\lambda^{-1}/\sqrt{B} = 4.49 \text{ meV}/T^{1/2}$ and $\lambda\sqrt{B} = 25.6 \text{ nm T}^{1/2}$) with published data³⁴ on width dependence of the effective Landé factor g^* , governing the Zeeman splitting $E_Z = g^* \mu_B B$ (for $W \geq 30 \text{ nm}$, it is $g^* = -0.44$ and $E_Z/B = 0.03 \text{ meV}/T$; in narrower wells, g^* increases, passing through zero at $W \approx 5.5 \text{ nm}$; recall that $w \approx W + 3 \text{ nm}$).

The most important phase boundary drawn in Fig. 3(c) divides the polarized and unpolarized $\nu_e = \frac{4}{11}$ states, i.e., the correlated QE and QE_R liquids at a finite $\nu = \frac{1}{3}$. In the experiment of Pan *et al.* in Ref. 1, the polarized $\nu_e = \frac{4}{11}$ state was observed in a symmetric $W = 50 \text{ nm}$ GaAs quantum well at $B = 11 \text{ T}$. The corresponding point (w, B) marked with a plus lies very close to the predicted phase boundary, suggesting that the experimentally detected polarization depended critically on the choice of a very wide well. Reference 31 reports identification of an incompressible $\nu_e = \frac{4}{11}$ state at a very high field $B = 33 \text{ T}$, taken as an argument for spin polarization. Indeed, the corresponding data point marked with a cross ($W = 30 \text{ nm}$ was assumed after Ref. 32) lies deep inside the predicted “QE liquid” phase area. The $\nu_e = \frac{4}{11}$ state was also observed³² in several other systems marked with dots and lying rather close to the predicted phase boundary. However, no clear evidence for an unpolarized $\nu_e = \frac{4}{11}$ has yet been reported.

It is clear from Fig. 3(c) that the spin transition in narrower wells shifts quickly to higher magnetic fields [i.e., to higher electron concentrations $\rho_e = \nu_e(2\pi\lambda^2)^{-1}$], especially when the width dependence of g^* is taken into account. This suggests that the spin transition at $\nu_e = \frac{4}{11}$ might be confirmed in an experiment similar to Ref. 1, carried out in a sample with the same W and ρ_e but with the layer width w tuned by the electric gates (inducing a controlled well asymmetry).

The role of QP interaction in stabilizing the QE_R phase is clear from the comparison of boundaries dividing correlated QE/QE_R liquids and noninteracting QE/QE_R gases (the gas occurs at $\nu \ll \frac{1}{3}$, with the critical equation $\Delta\varepsilon = E_Z$; the CF gas \leftrightarrow liquid transition was recently demonstrated by inelastic light scattering³⁵). Additional boundaries [not shown here, but see Fig. 13(b) in Ref. 20] appear at even smaller B , defining the areas of stability for a gas of CF skyrmions of different sizes.^{18–20,36} Note also that $\Delta\varepsilon$ is determined more accurately than Δu , possibly explaining the incorrect position of the experimental point inside the predicted QE gas and/or QE_R liquid area.

Let us also note that crossing the phase boundary (e.g., by applying an additional parallel magnetic field) might not necessarily cause an instantaneous phase transition. This is because the competing spin phases are macroscopically different, and flipping the first single spin might take more energy. In other words, the mixed QE/QE_R liquids might have (at the phase boundary) higher energy than both the pure QE and QE_R states. This scenario, analogous to the supercooling or superheating in a gas-liquid transition, must be taken into account when interpreting experimental results in tilted magnetic fields.

VII. CONCLUSION

By combining composite fermion theory with exact numerical diagonalization, we studied two spin states of the

second-generation incompressible quantum liquid at $\nu_e=\frac{4}{11}$. Our main result is prediction of a transition between these competing states, different not only by the spin polarization but also by the microscopic mechanism of incompressibility (the nature of CF-CF correlation). Starting with effective interaction pseudopotentials of polarized and reversed-spin Laughlin quasielectrons (QE and QE_R), we determined their correlation energies u in conditions adequate for realistic 2D electron layers of different widths w and in different magnetic fields B . This allowed us to draw a spin phase diagram of the $\nu_e=\frac{4}{11}$ state in the (w, B) coordinates. Comparison of our numerics with the experiments of Pan *et al.* is not conclusive. In particular, it seems that the effect of the CF-CF interaction and correlation on the spin phase boundary might be overestimated in the present model (with a likely origin in the limited accuracy of the quantitative estimate of the

CF-CF pseudopotentials in Fig. 2). However, our prediction of the spin transition induced in the same quantum well by external electric gates offers a possibility of more accurate testing of the theory. Hall measurements in the samples lying deeper inside the predicted QE_R liquid phase area might also be insightful. Finally, in constructing the phase diagram, we only considered the extreme polarizations of $P=100\%$ and 50% , leaving out the possibility of mixed QE/QE_R states near the predicted phase boundary.

ACKNOWLEDGMENTS

The authors thank Wei Pan for helpful discussions and sharing unpublished experimental data and acknowledge partial support from Grants No. DE-FG 02-97ER45657 of U.S. DOE and No. N202-071-32/1513 of the Polish MNiSW.

-
- ¹W. Pan, H. L. Störmer, D. C. Tsui, L. N. Pfeiffer, K. W. Baldwin, and K. W. West, Phys. Rev. Lett. **90**, 016801 (2003).
²R. B. Laughlin, Phys. Rev. Lett. **50**, 1395 (1983).
³D. C. Tsui, H. L. Störmer, and A. C. Gossard, Phys. Rev. Lett. **48**, 1559 (1982).
⁴D. Yoshioka, *The Quantum Hall Effect* (Springer-Verlag, New York, 2002); *Perspectives in Quantum Hall Effects*, edited by S. Das Sarma and A. Pinczuk (Wiley, New York, 1997); T. Chakraborty and P. Pietiläinen, *The Fractional Quantum Hall Effect* (Springer, Heidelberg, 1988).
⁵J. K. Jain, Phys. Rev. Lett. **63**, 199 (1989); Science **266**, 1199 (1994); Phys. Today **53** (4), 39 (2000).
⁶J. H. Smet, Nature (London) **422**, 391 (2003).
⁷C. C. Chang and J. K. Jain, Phys. Rev. Lett. **92**, 196806 (2004); M. R. Peterson and J. K. Jain, *ibid.* **93**, 046402 (2004).
⁸A. Lopez and E. Fradkin, Phys. Rev. B **69**, 155322 (2004).
⁹A. Wójs, K.-S. Yi, and J. J. Quinn, Phys. Rev. B **69**, 205322 (2004); A. Wójs, D. Wodziński, and J. J. Quinn, *ibid.* **71**, 245331 (2005).
¹⁰M. O. Goerbig, P. Lederer, and C. M. Smith, Phys. Rev. Lett. **93**, 216802 (2004); Phys. Rev. B **69**, 155324 (2004).
¹¹A. Wójs, D. Wodziński, and J. J. Quinn, Phys. Rev. B **74**, 035315 (2006).
¹²J. J. Quinn and J. J. Quinn, Solid State Commun. **140**, 52 (2006).
¹³B. I. Halperin, Helv. Phys. Acta **56**, 75 (1983).
¹⁴T. Chakraborty and F. C. Zhang, Phys. Rev. B **29**, 7032 (1984); F. C. Zhang and T. Chakraborty, *ibid.* **30**, 7320 (1984); T. Chakraborty, P. Pietiläinen, and F. C. Zhang, Phys. Rev. Lett. **57**, 130 (1986).
¹⁵E. H. Rezayi, Phys. Rev. B **36**, 5454 (1987); **43**, 5944 (1991).
¹⁶X. G. Wu, G. Dev, and J. K. Jain, Phys. Rev. Lett. **71**, 153 (1993).
¹⁷V. M. Apalkov, T. Chakraborty, P. Pietiläinen, and K. Niemelä, Phys. Rev. Lett. **86**, 1311 (2001).
¹⁸R. K. Kamilla, X. G. Wu, and J. K. Jain, Solid State Commun. **99**, 289 (1996).
¹⁹A. H. MacDonald and J. J. Palacios, Phys. Rev. B **58**, R10171 (1998).
²⁰A. Wójs and J. J. Quinn, Phys. Rev. B **66**, 045323 (2002).
²¹C. C. Chang, S. S. Mandal, and J. K. Jain, Phys. Rev. B **67**, 121305(R) (2003).
²²A. Wójs and J. J. Quinn, Phys. Rev. B **61**, 2846 (2000).
²³S. S. Mandal and J. K. Jain, Phys. Rev. B **66**, 155302 (2002).
²⁴K. Park and J. K. Jain, Phys. Rev. B **62**, R13274 (2000).
²⁵I. Szlufarska, A. Wójs, and J. J. Quinn, Phys. Rev. B **64**, 165318 (2001).
²⁶F. D. M. Haldane, Phys. Rev. Lett. **51**, 605 (1983).
²⁷G. Fano, F. Ortolani, and E. Colombo, Phys. Rev. B **34**, 2670 (1986).
²⁸F. D. M. Haldane, in *The Quantum Hall Effect*, edited by R. E. Prange and S. M. Girvin (Springer-Verlag, New York, 1987), Chap. 8, pp. 303–352.
²⁹S.-Y. Lee, V. W. Scarola, and J. K. Jain, Phys. Rev. Lett. **87**, 256803 (2001); Phys. Rev. B **66**, 085336 (2002).
³⁰P. Sitko, K.-S. Yi, and J. J. Quinn, Phys. Rev. B **56**, 12417 (1997).
³¹W. Pan, H. L. Störmer, D. C. Tsui, L. N. Pfeiffer, K. W. Baldwin, and K. W. West, Int. J. Mod. Phys. B **16**, 2940 (2002).
³²W. Pan (private communication).
³³A. Wójs, Phys. Rev. B **63**, 125312 (2001).
³⁴M. J. Snelling, G. P. Flinn, A. S. Plaut, R. T. Harley, A. C. Tropper, R. Eccleston, and C. C. Phillips, Phys. Rev. B **44**, 11345 (1991).
³⁵Y. Gallais, T. H. Kirschenmann, I. Dujovne, C. F. Hirjibehedin, A. Pinczuk, B. S. Dennis, L. N. Pfeiffer, and K. W. West, Phys. Rev. Lett. **97**, 036804 (2006).
³⁶D. R. Leadley, R. J. Nicholas, D. K. Maude, A. N. Utjuzh, J. C. Portal, J. J. Harris, and C. T. Foxon, Phys. Rev. Lett. **79**, 4246 (1997).